AN EXAMPLE OF SEQUENTIAL LETHALITY MODELS: DEBRIS PENETRATION INTO CONVENTIONAL BUILDINGS

by

David D. Bogosian, Karagozian & Case
John E. Crawford, Karagozian & Case
James B. Baeker, ACTA Inc.

Abstract

This paper summarizes an approach developed for obtaining quantitative vulnerabilities of buildings and their occupants exposed to falling debris, depending on (1) the fragment size, weight, and velocity, (2) the structural characteristics of the building roof and floors, and (3) the occupancy level of each floor of the building. The penetration model developed provides an example of the complexity that component lethality models must have to include the propagation of hazardous threats through the interior of a facility. The model is generic and can accommodate wood, steel, and concrete structural members. Kinetic energy of the impacting fragment is assumed to be fully transferred into the structural system, and the resulting response is computed using a simplified engineering model that includes both shear and flexural failures. The fragment's residual velocity after passing through each level is computed using conservation of energy methods to allow sequential treatment of all floors in a building. The hazard area resulting from fragment penetration is calculated probabilistically and, when combined with the floor occupancy, is used to produce an expected number of casualties for each impact. Sample results are presented to illustrate parametric sensitivities and potential areas of application.

Overview of Lethality Models

Current interest in the vulnerability of buildings to various types of explosive- or accident-generated environments has focused attention on lethality models which can predict building damage and casualties from a given scenario. One of the areas of greatest difficulty in implementing these models is the propagation of the various hazards (fragments, blast, shock, chemical, biological, or radioactive agents, heat, smoke, etc.) into the interior of the facility. As a result, current lethality models are generally limited to the intial interaction at the building's perimeter and are unable to propagate the hazards into various parts of the building's interior.

These hazards require consideration as potential threats in the context of missile and space booster launch accidents, aircraft accidents, terrorism, military conflict, or explosive safety. Quantitative prediction of lethality is desirable for both design and assessment purposes and for decision makers. Given the large uncertainties in building configuration, distribution of personnel over the building, and hazard levels, these predictions are most appropriately provided in probabilistic terms. Since this typically involves some level of Monte Carlo simulation, the models embedded within the assessment tool must execute with sufficient speed to permit large numbers of cases to be analyzed in a relatively short span of time. Figure 1 shows some of the components required in the lethality model and their role in obtaining the lethality estimates desired.

Report Documentation Page

Form Approved
OMB No. 0704-0188

1. REPORT DATE **AUG 1996**	2. REPORT TYPE	3. DATES COVERED **00-00-1996 to 00-00-1996**

4. TITLE AND SUBTITLE **An Example of Sequential Lethality Models: Debris Penetration into Conventional Buildings**	5a. CONTRACT NUMBER
	5b. GRANT NUMBER
	5c. PROGRAM ELEMENT NUMBER
6. AUTHOR(S)	5d. PROJECT NUMBER
	5e. TASK NUMBER
	5f. WORK UNIT NUMBER
7. PERFORMING ORGANIZATION NAME(S) AND ADDRESS(ES) **Karagozian & Case,625 N. Maryland Avenue,Glendale,CA,91206-2245**	8. PERFORMING ORGANIZATION REPORT NUMBER
9. SPONSORING/MONITORING AGENCY NAME(S) AND ADDRESS(ES)	10. SPONSOR/MONITOR'S ACRONYM(S)
	11. SPONSOR/MONITOR'S REPORT NUMBER(S)

12. DISTRIBUTION/AVAILABILITY STATEMENT
Approved for public release; distribution unlimited

13. SUPPLEMENTARY NOTES
See also ADM000767. Proceedings of the Twenty-Seventh DoD Explosives Safety Seminar Held in Las Vegas, NV on 22-26 August 1996.

14. ABSTRACT
see report

15. SUBJECT TERMS

16. SECURITY CLASSIFICATION OF:			17. LIMITATION OF ABSTRACT	18. NUMBER OF PAGES	19a. NAME OF RESPONSIBLE PERSON
a. REPORT **unclassified**	b. ABSTRACT **unclassified**	c. THIS PAGE **unclassified**	**Same as Report (SAR)**	**20**	

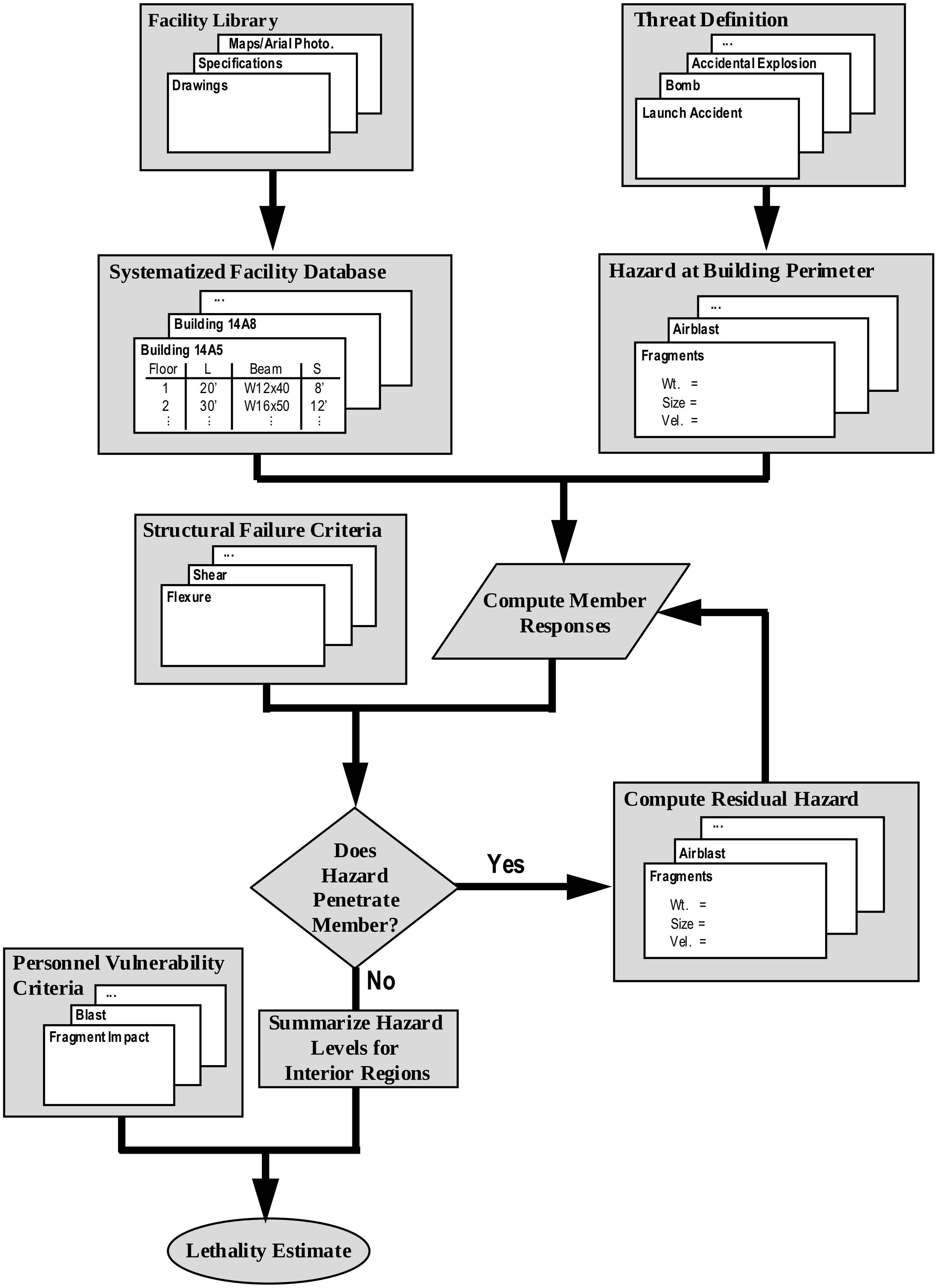

Figure 1. Components of a lethality model.

For example, there are models capable of computing the blast vulnerability of an exterior wall/frame system,[1] but should the exterior walls fail there is no provision for propagating the airblast beyond these walls and into the building's interior. Certainly, this propagation is a highly complex phenomenon that remains intractable even for high-powered first principle finite element codes, but the limitation is not overly constraining so long as the building being analyzed is relatively small and devoid of interior partitions. However, particularly when the building is large and the explosive source is small and close in, such a model will predict localized failure of the exterior wall facing the charge and survival of all other elements; what can then be concluded about the fate of the building's occupants? It is relatively easy to predict the extent of failure of the exterior walls, but what does this imply about occupant casualties? It is likely that the occupants in the distant portions of the building are shielded from blast effects by the cumulative effect of the interior walls. Even relatively flimsy construction and building contents (e.g., metal studs with drywall, office furniture) can act to absorb fragment loads and attenuate blast loads, particularly if there are many partitions and the distance of propagation is large. Both the above conditions apply to a typical office building, and the attenuative effect is greatly enhanced if the interior walls are load-bearing, such as concrete masonry or reinforced concrete. In many cases, the strength of the exterior wall may well be sufficient to absorb the blast and fragment effects without any further propagation, even though the wall itself may collapse.

Figure 2 shows a hypothetical scenario with a small charge close to one side of a large building with interior masonry walls. The exterior walls fail opposite the charge but they also reduce the peak pressures by a significant margin. The next set of masonry walls will also fail and reduce the pressures even further. Thus, the corridor areas will remain vulnerable but the cubicles in the NW and NE corners would be protected since the masonry walls would be able to survive the reduced loading. Similarly, while the masonry wall on the west side of the SE quadrant (facing the corridor) would fail, the pressure level within the first row of cubicles would be low enough that the partition walls would be able to contain the blast, and the second and third rows of cubicles would survive. By comparison, analysis using models limited to exterior elements would be unable to make quantitative conclusions regarding casualties for occupants.

The portion of the flowchart in Figure 1 that has heretofore been neglected is the "computation of residual hazard" due to its inherent complexity. However, without some attempt at defining this propagation, models are limited to relying on using the response of exterior elements to provide any quantitative results for the interior of a building. The model presented in this paper takes an initial step at quantifying the interaction between environment and structure for a particular class of problem—debris falling onto a conventional building and penetrating through the roof and floor structures—and includes a simple yet physically logical approach for obtaining the residual environment—in this case, the residual velocity of the fragment as it passes through successive floors. The general approach, however, would be the same if the problem of interest was airblast, thermal, shock, or any other hazard to personnel or equipment.

[1] A prime example is the FACEDAP code (Facility and Component Explosive Damage Assessment Program) developed by the Southwest Research Institute for the U.S. Army Corps of Engineers, Omaha District, CEMRO-ED-ST.

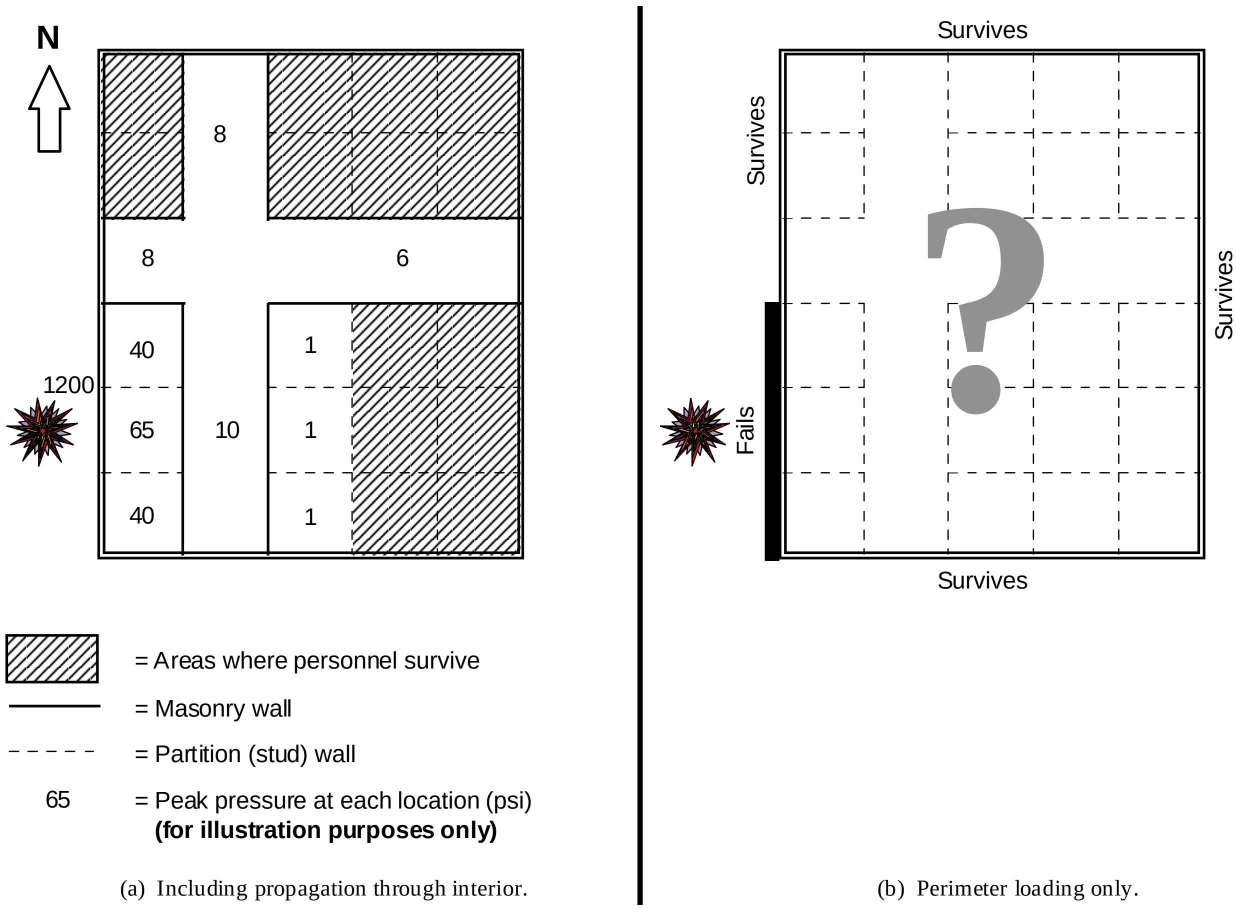

Figure 2. Hypothetical scenario illustrating effect of interior partitions on blast propagation and personnel survival.

Taken together, a number of such models can, in theory, be assembled to provide a comprehensive lethality assessment tool usable for providing quantitative hazard data for use by decision makers, planners and policy makers, designing new facilities, and evaluating retrofit concepts for existing facilities. The structure of the debris penetration model described in this paper provides an example of how such models can be assembled from individual components, each of which can be easily enhanced if better models become available.

Scope of Penetration Model

The context for the penetration model discussed herein is that of risk assessments for missile and space booster vehicle launch accidents. As a result of previous analytical and empirical studies,[2] data is available defining the number, size, and velocity of fragments generated by a particular launch failure scenario, along with the probability of that scenario occurring. Because the space vehicle's mass, configuration, and environment is constantly changing (because of fuel being burned, stages being jettisoned, and changes in altitude and

[2] One of numerous examples is "LARA Vehicle Specific Data Bases, FY95 Revision", J. Baeker and M. Herndon, ACTA Inc., September 1995 (Technical Report No. 95-314/72-02).

velocity), the distribution of fragments is highly dependent on the time after liftoff that the failure occurs. Also, depending on the prevailing weather patterns (wind velocities and directions), the footprint of the debris on the ground will be highly variable. However, if the impact distributions for the various categories of fragments can be predicted, the probability of a given fragment impacting a given building can be computed. The above computations are performed within the LARA program[3] whose scope covers a broader range of hazards than merely fragment penetration. The penetration model (named HACK for Hazard Area Computational Kernel) is then called upon to estimate the probabilistic hazard area on each floor of the building where casualties would be incurred by personnel located within the area. When combined with data on the population density of each floor, the total number of casualties can be estimated for that particular fragment impacting that particular building. The process (illustrated in Figure 3) is repeated for all combinations of fragments and buildings. When combined with the population densities, probabilities of impact and of that particular launch failure scenario, and repeated for all possible failure scenarios, the probabilistic expected number of casualties for a given launch event is computed.

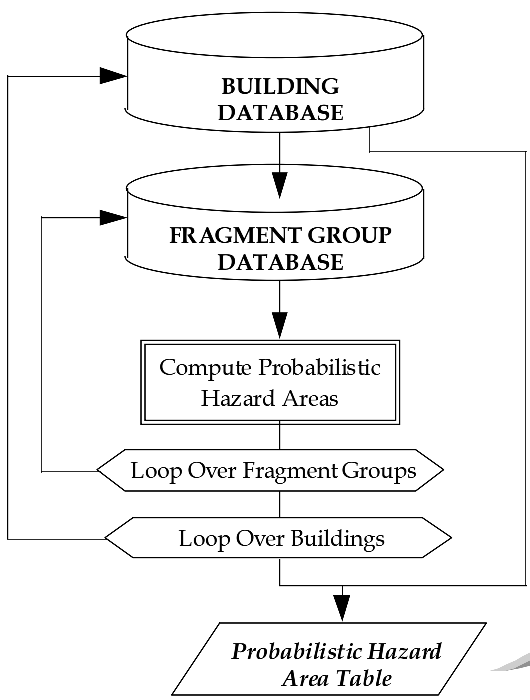

Sample Hazard Area Table
(areas in sq. ft.)

	Building 1		Building 2 ...
Fragment Group	Floor 1	Floor 2	Floor 1 ...
1	45	8.4	3.2
2	8.0	0.5	0.0
3	235	32	9.9
M	M	M	M

Figure 3. Overview of model utilization.

The objective of the HACK lethality model is thus the calculation of the hazard area for each floor of the building. The required inputs are as follows:

For the fragment: • Mass

[3] Documented in "Launch Risk Analysis Program: Mathematical Methodology and Functional Flow Diagrams", Revision V, NTS Engineering, Long Beach, CA, September 1986 (Technical Report No. 86-3148-03). Periodic updates are provided in other documents such as "Debris Risk Analysis: Model Developments, FY95 Activities", ACTA Inc., Torrance, CA, September 1995 (Report No.k 95-314/71-01).

- Velocity at impact
- Projected area (treated probabilistically, hence a range is actually input)

For the building:
- Dimensions (overall length/width, member spacings, etc.)
- Member properties (e.g., beam section properties, etc.)
- Number of stories

The primary output consists of a single number, the hazard area in square feet, for each story in the building for a given fragment impact. The entire model has been implemented into a FORTRAN module which can run as a stand-alone program in batch mode or as a module within a larger program.

A few features of the model merit further comment. Given the variety of building and fragment types, it was necessary that the idealizations of both be kept relatively generic to accommodate this variety. The individual components of the lethality model (e.g., beam response computation, residual velocity computation, etc.) are highly modularized, both in the logic utilized as well as in the coding, to facilitate potential future enhancement at a later date with additional or more sophisticated modules. Finally, given the large numbers of buildings which needed to be analyzed, it was important that the level of input required to define a building be limited to a few values easily obtainable from typically available structural drawings. Similarly, the large number of fragments mandated limiting input values for the fragment to the basic quantities of mass, area, and velocity.

Model Idealizations and Simplifications

In order to enable the model to execute in relatively rapid fashion and satisfy the constraints described above, a number of idealizations and simplifications were required to keep the scope of the problem manageable. This was especially true in light of the wide range of building and fragment types that HACK was required to handle. Wherever the actual structural response had to be simplified, conservative assumptions were made; that is, the simplification *maximized* the resulting hazard area. The list below enumerates the primary idealizations made, separating them into the two chief elements treated, the building and the fragment.

Building Idealization (please refer to Figure 4)

- The building footprint is rectangular and constant over all floors. [Non-rectangular buildings can be treated by dividing them into rectangular pieces; buildings which have different footprints at different levels could be treated similarly.]
- The framing in the roof/floor consists of three sets of members: girders (large beams spanning between columns or exterior walls), joists (smaller beams spanning between girders), and plate (two-dimensional sheathing such as corrugated steel decking, concrete slabs, plywood, etc.).
- All joists and girders are evenly spaced throughout the roof/floor area.
- The roof is flat and horizontal, so that the fragment’s vertical velocity component will be used in the analysis.

- Separate properties are allowed for the roof and the floors, but all floors must be identical (same members, spacings, etc.). [Inclusion of varying floor definitions is easily implemented but complicates the input and is not likely to occur much in typical construction.]
- Penetration is controlled by the horizontal framing members (girders, joists, plate) and not by any vertical load-bearing members (columns, bearing walls). [The model could incorporate a separate set of modules to permit analytical treatment of vertical load-bearing members; however, this would greatly increase the complexity of the model and lay beyond the scope of the current effort.]
- Structural members have a binary damage state: failed or not failed. If the latter, the hazard area is zero and the fragment does not penetrate to the next floor; if the former, there is a non-zero hazard area and the fragment will reach the next floor with some residual velocity. No intermediate damage states (e.g., moderate damage where the fragment does not penetrate but causes sufficient damage to the member to generate some secondary debris, such as concrete spallation) are considered.

Fragment Idealization

- The fragment is inert, i.e., non-explosive, and the only energy it imparts to the building is its kinetic energy.
- The fragment is rigid and non-deformable; thus, upon impact, all of its kinetic energy is transferred into the structural element and none goes into deforming the fragment. [In reality, the amount of interaction between fragment and building will vary as a function of their relative stiffnesses and the detailed distribution of mass and stiffness within the fragment, details which are currently not included in the fragment database. Fragment deformation could prove to be a significant energy absorbing mechanism; however, the current assumption is conservative and believed reasonable.]
- A corollary of the above is that the fragment doesn't change size or mass as it passes through successive floors. [In reality, some attrition of its mass is likely to occur and can be incorporated in a simple way by putting in a factor of some kind; the current assumption is conservative, at least with regard to the mass.]
- The fragment impact area A_{frag} is treated probabilistically by using a uniform distribution from its minimum to its maximum values; this accounts for the varying projected area presented by a rotating body, as shown in Figure 5.
- The loaded area upon impact is a square of size $D_{frag} = \sqrt{A_{frag}}$. [The actual area could vary widely, both in shape as well as in aspect ratio, but anything other than a square would vastly increase the model's complexity.]
- The probability of fragment impact is uniform over the entire footprint of the building. This is reasonable given the wide area covered by the debris impact distribution.

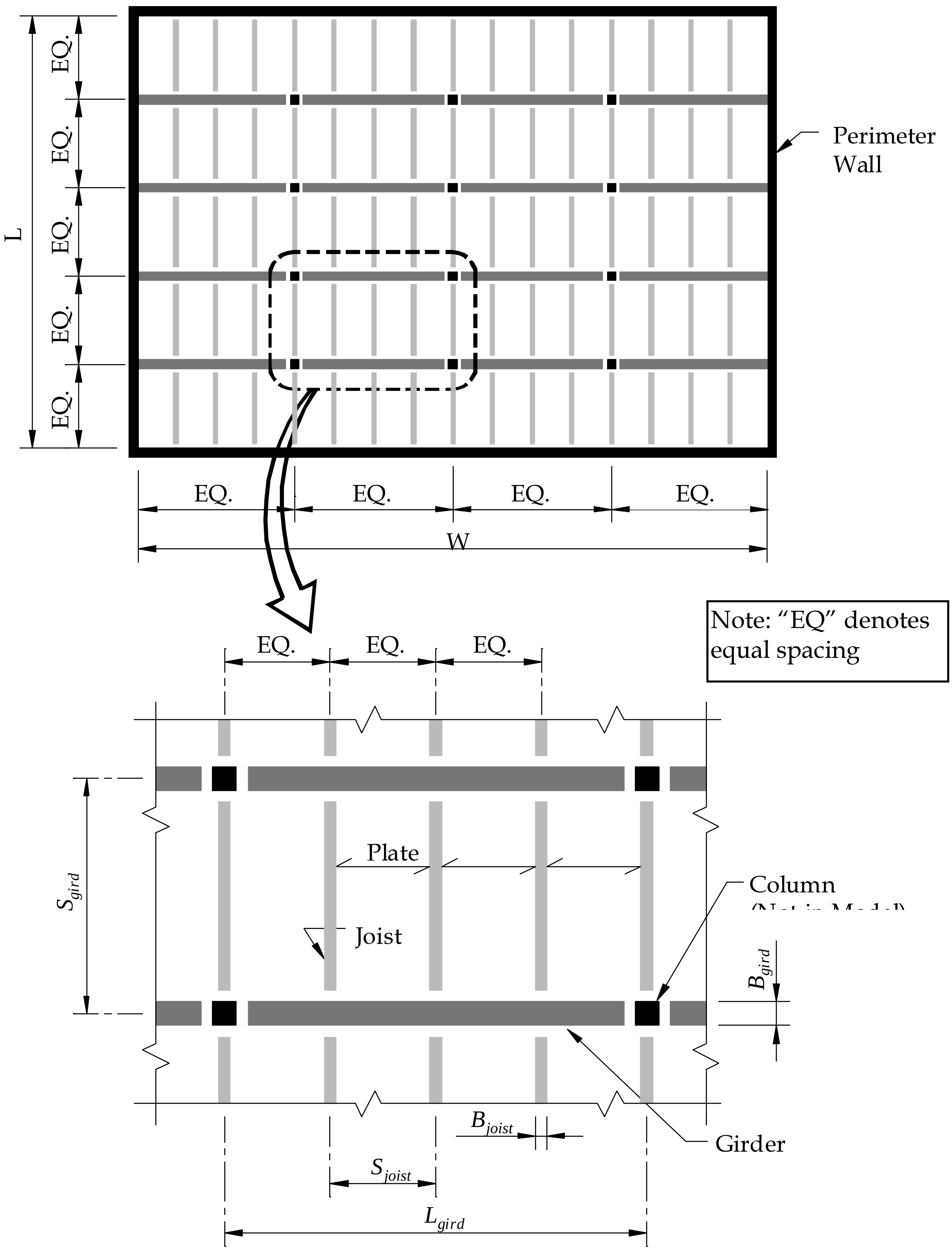

Figure 4. Idealization of building elements and dimensions.

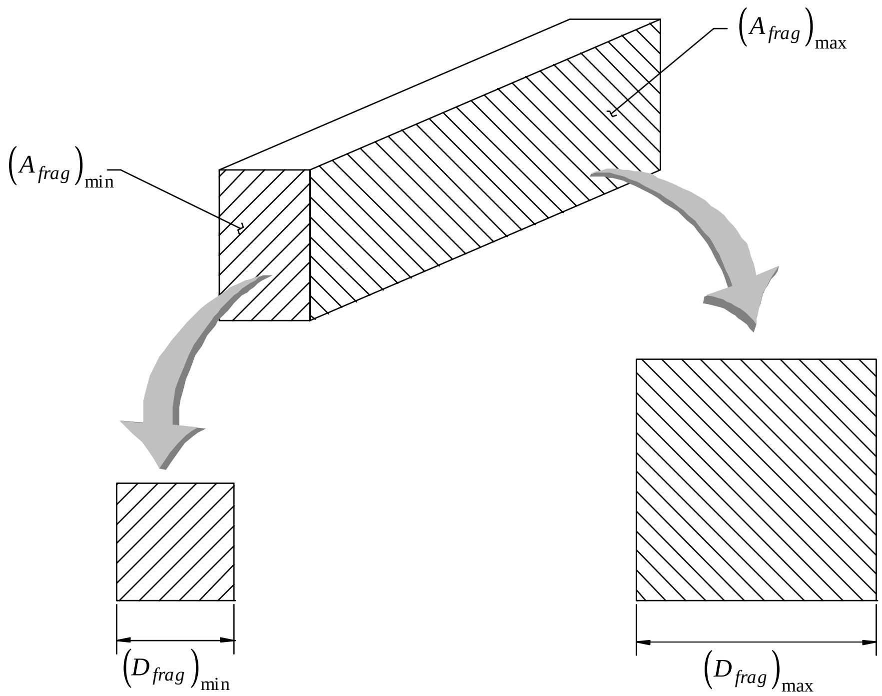

Figure 5. Idealized fragment areas and impact areas.

Model Logical Structure

The structure of the HACK lethality model consists of a number of nested loops, each covering one of the primary parameters being treated, as illustrated in Figure 6. The outermost loop addresses the variability in the fragment area and, therefore, the size of the square loaded area; a total of 5 equally spaced samples are used over the range from $(A_{frag})_{min}$ to $(A_{frag})_{max}$ to provide variation without excessive computational effort. Next, for each fragment, the building stories are treated sequentially from top to bottom.

At this point, a given fragment (with known properties) is impacting a given roof/floor structure (with known properties). However, we must account for the variability of impact location: the fragment could land directly on top of a girder, over a joist, or on the plate; furthermore, the likelihood of its penetration depends greatly on which of those members it hits. The probability of impacting any given member will depend on the member dimensions and the size of the fragment: larger fragments will never hit the plate since they're too big to fit between joists (i.e., they cannot penetrate the plate without failing the joists, therefore only joist failure need be considered), and similarly the number of joists or girders being hit depends on fragment size. Consequently, four cases were defined depending on the relative dimensions of the fragment and roof/floor structure. For each one, the possible impact conditions (IC's) were defined, each corresponding to the type and number of structural members with which the fragment interacts:

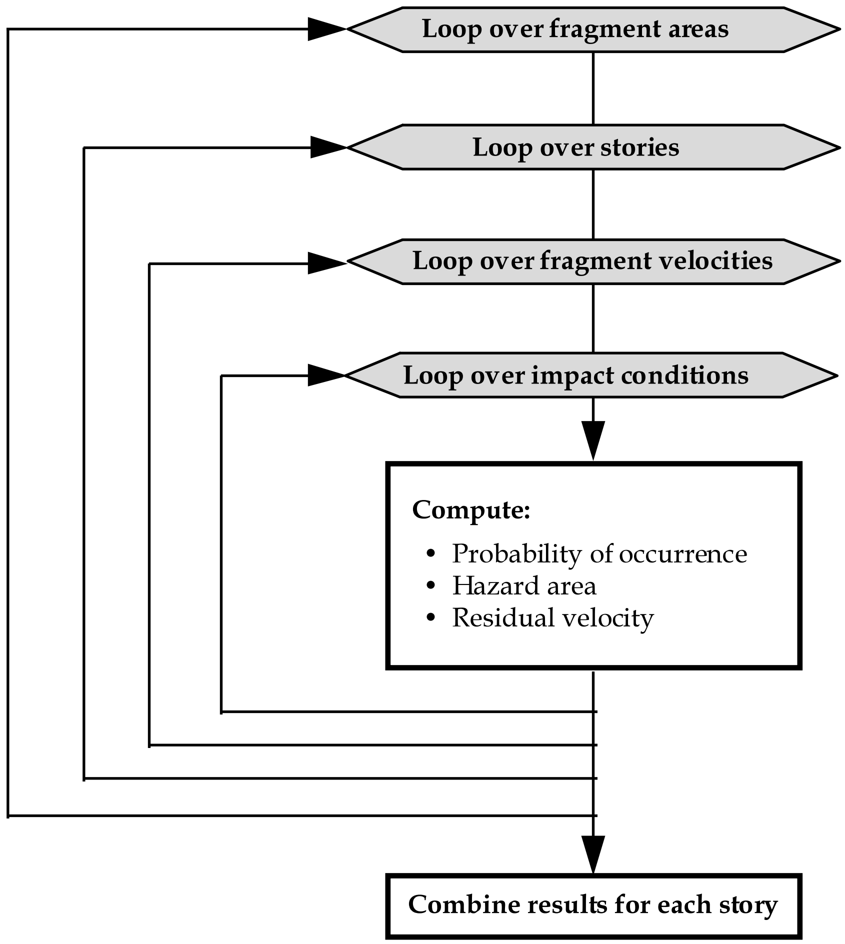

Figure 6. Overall structure of model.

1. Small fragment that fits between joists; in this case, there are 3 IC's: (a) plate, (b) joist, or (c) girder.

2. Medium fragment larger than the joist spacing (hence can't hit the plate alone) but smaller than the girder spacing; here, there are also 3 IC's: (a) N_j joists[4], (b) N_j-1 joists, (c) one girder.

3. Large fragment, larger than the joist span but able to fit between columns; here there are only 2 IC's: (a) N_g girders[4], (b) N_g-1 girders.

4. Very large fragment that is unable to fit between columns; for this case, there is only one IC.

To illustrate the combinations available, Figure 7 shows the areas associated with each IC for case 1, the case corresponding to a very small fragment. Conceptually, as the fragment size is

[4] Note that N_j, is the maximum number of joists impacted and is computed as a function of the fragment size and the joist spacing. Similarly, N_g is the number of girders impacted.

reduced to a pinpoint, the area for IC=2 (joist impact) reduces to the area of the joists alone; conversely, as the fragment size approaches the joist spacing, the area associated with plate impact (IC=1) nearly disappears. Since all the building dimensions and spacings are known, the sketch is used to compute the total area associated with each IC which, when divided by the total floor area, gives the probability of that particular IC occurring. Similar figures can be drawn for the other cases.

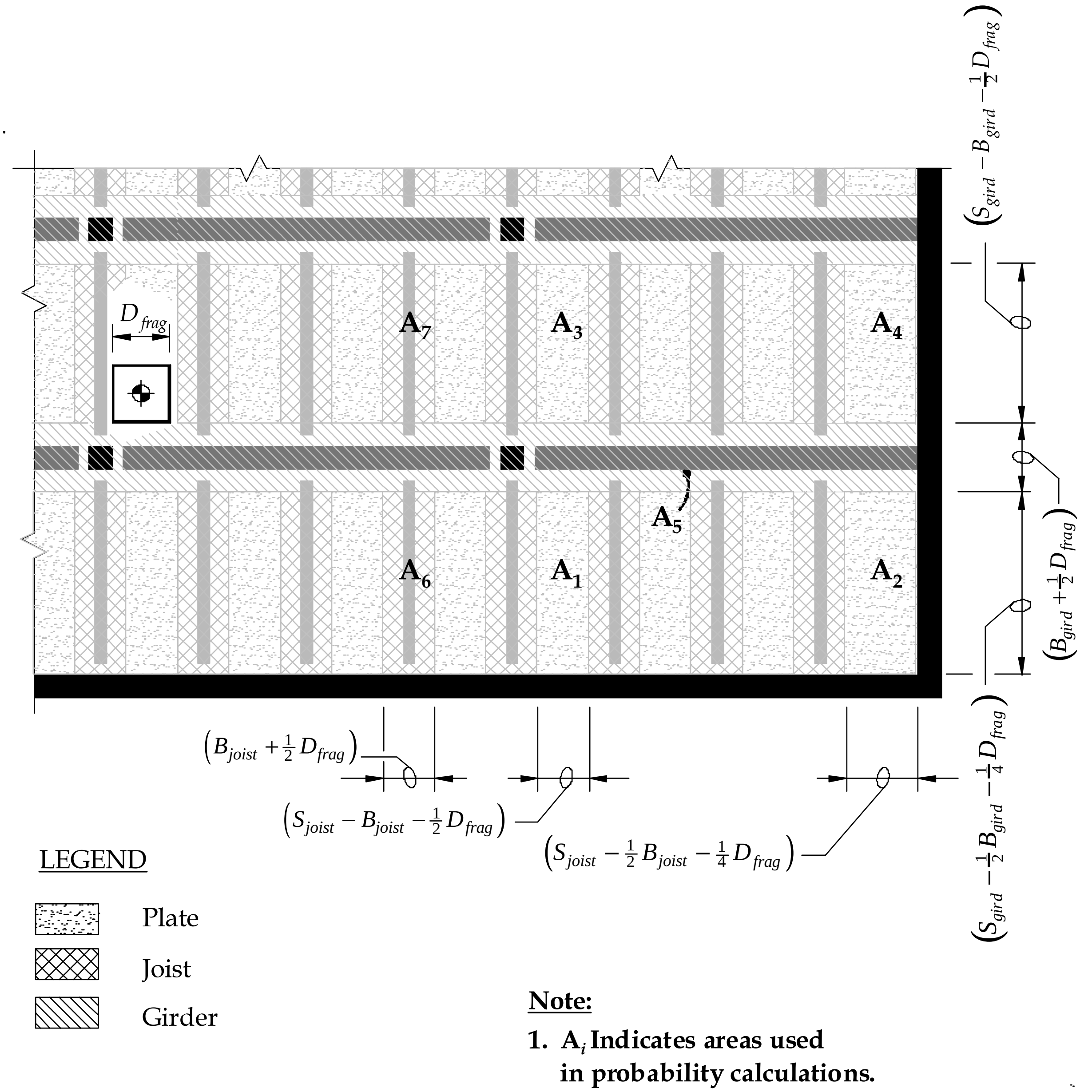

Figure 7. Impact conditions for case 1: small fragment.

Since each IC results in the fragment interacting with different structural members (with different resistance to impact loads), it follows that the residual velocity of the fragment will be

different for each IC. Consequently, when the analysis progresses from the roof to the topmost floor, the number of velocities is increased from 1 to 2 (if the roof had 2 IC's). Similarly, if the topmost floor has 3 IC's, the number of possible velocities impacting the second topmost floor is 2x3=6. This cascading propagation of impact velocities is illustrated in Figure 8; in the worst case, if there are 3 IC's per floor (the maximum possible), the analysis of the bottom floor of an N-story building would involve $3^{(N-1)}$ velocities. This exponential relationship results in lengthy run times for any buildings with more than a few stories, but is unavoidable if the propagation of the hazard (in this case, the fragment velocity) is to be represented in a systematic fashion.

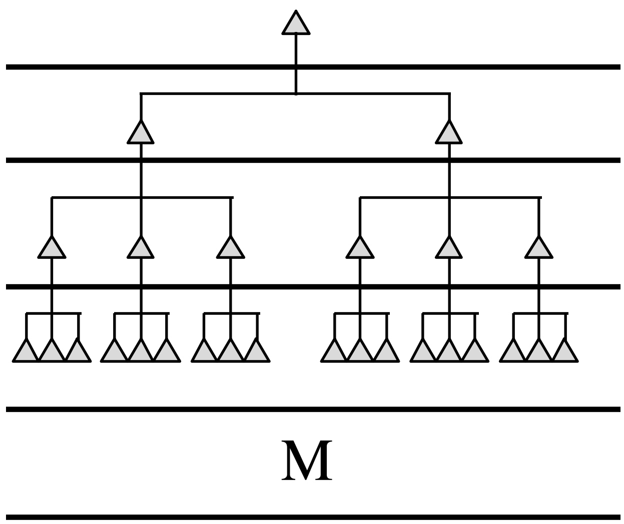

Level	# of IC's	# of vel's
1	2	1
2	3	2
3	3	6
4	3	18
N	$(NIC)_N$	$\prod_{i=1}^{N-1}(NIC)_i$

Note: $(NIC)_N$ = number of impact conditions for Nth level

Figure 8. Cascading increase in number of impact velocities at each level.

We now return to the flow chart in Figure 6; for a given fragment area and a given story, the next loop (third from the top) is over the individual impact velocities possible. For each velocity, the final loop is over the number of impact conditions possible. For each combination of these parameters, then, the model must compute three values: (a) the probability of that IC occurring, (b) the hazard area associated with that IC, and (c) the residual velocity of the fragment if it succeeds in penetrating the member. While (a) is easily computed from the building parameters and fragment size, (b) and (c) constitute the heart of the module and are defined in greater detail below.

The final computation of hazard area includes a number of probability terms, as shown in the equation below:

$$HA_{tot}(M,N) = \sum_i \left\{ P'(i)\, P'_{fail}(i) \left[\sum_j \; HA\,(j) \cdot P(j) \cdot P_{fail}(j) \right] \right\}$$

Here, HA_{tot} is the total hazard area for the M^{th} fragment area (ranging from 1 to 5) and the N^{th} level of the building. The inner bracket encloses a sum (over all the impact conditions being analyzed) of the product of (1) the probability P of that IC, (2) the probability P_{fail} that the member failed, and (3) the hazard area HA associated with failure of that member. The sum in the inner brackets then represents the hazard area at that level *if the fragment penetrated far enough to reach the level in question*. Consequently, a second term must be applied, represented by the product in the outer sum in curly braces, which accounts for the probability that fragment reached the level being analyzed. Thus, the outer sum is taken over all the impact velocities at that level, each of which has a probability P' of occurring and a probability P'_{fail} of having failed.

Member response

Since the model covers three different building materials (steel, concrete, wood), two types of members (plates and joists/girders), and two response modes (shear and bending), a total of 12 individual response models are needed. The types of models currently utilized are summarized[5] in Table 1. Bending response is calculated using a single degree of freedom (SDOF) approach which is computationally efficient yet represents the dominant physical characteristics of the system. The basic SDOF model (illustrated in Figure 9) requires definition of a few easily obtained parameters (mass, elastic stiffness, yield resistance, load/mass factor) which in turn can be computed from the model input. An SDOF model was also used to obtain the shear response of concrete and steel joist/girders, but the shear calculation was terminated at the time of hinge formation observed in the bending calculation, since once the beam has plasticized the mechanism for shear transfer to the supports is no longer viable. In all cases where SDOF's were used, the peak deflection was computed and compared to well-established criteria for failure (typically defined as a percentage of the span) to determine whether or not the element failed.

Table 1. Overview of response models utilized.

	Bending	***Shear***		
	(all materials)	Steel	Concrete	Wood
Joist/Girder	SDOF	SDOF	SDOF	Shear energy comparison
Plate	SDOF (1-way)	Empirical model	Shear energy comparison	Shear energy comparison

Since the actual time history of load during impact is a function of the fragment's detailed configuration and beyond the scope of the current model, the model (conservatively) assumes that the fragment momentum is completely imparted to the structural element. Thus, the initial velocity of the lumped mass in the SDOF model can be easily estimated and applied as an initial condition to the calculation.

[5] Considerably more detail regarding the response models (equations and procedures used to obtain the various parameters needed, references for key equations, intricacies of logic utilized, failure criteria, etc.) can be found in the HACK documentation, "Hazard Area Computational Kernel: A Model for Predicting Fragment Penetration into Buildings", D. Bogosian, Karagozian & Case, Glendale, CA, July 1996 (Technical Report No. TR-96-29).

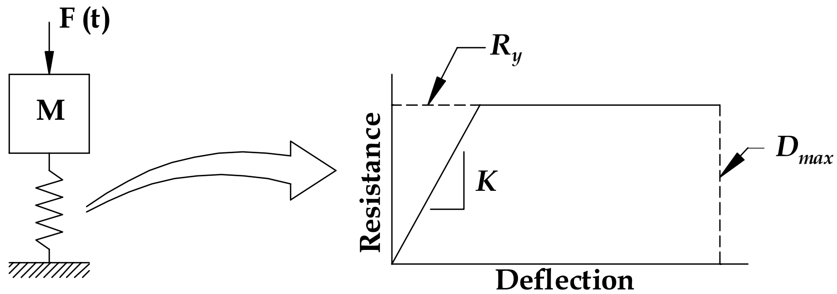

Figure 9. SDOF model parameters.

As generic as the SDOF model is, some response modes were not amenable to such a representation and alternative response prediction methods were implemented. For shearing of steel plate, an empirically based model (consisting of a closed-form equation which gives the velocity required to penetrate a given thickness of steel for a given set of fragment characteristics) was utilized. For shearing of wood joists/girders and concrete or wood plates, the total internal energy required to fail the structural material in shear (essentially the area under the stress-strain curve) was computed and compared to the fragment's kinetic energy; if the fragment energy exceeded the required shear energy, punch-through was assumed to occur.

Since actual material properties (strength, modulus of elasticity) are not likely to be easily obtained, especially when analysis of thousands of facilities is envisioned, the model assumes typical material properties (e.g., a concrete compressive strength of 4,000 psi, wood shear strength of 100 psi, etc.) in defining the needed SDOF and shear energy parameters.

One problem with using the SDOF model to do bending calculations is that the system characteristics (stiffness, yield resistance) are highly dependent on the location of impact; in terms of the outcome, impact near midspan may result in failure while impact near the support may not. Hence, a set of 5 actual analyses were carried out for each beam to represent the distribution of possible impact points across the span (as shown in Figure 10), and the actual probability of failure was computed based on the number of points at which failure occurred. For example, if failure occurred at the two points nearest midspan but nowhere else, the probability of failure was 0.4 for that case, and was factored into the hazard area computation. The distribution of load was assumed to be uniform and equal to the fragment width, D_{frag}.

There remains to be computed the residual velocity of the fragment after it passes through the structural member. In general, this was done using conservation of energy methods with the assumption that the residual kinetic energy is equal to the original kinetic energy minus the energy absorbed by the structure. Thus, for SDOF models, the internal energy absorbed by the failed structural member can be estimated from the area under the load-deflection curve, and the residual velocity computed as follows:

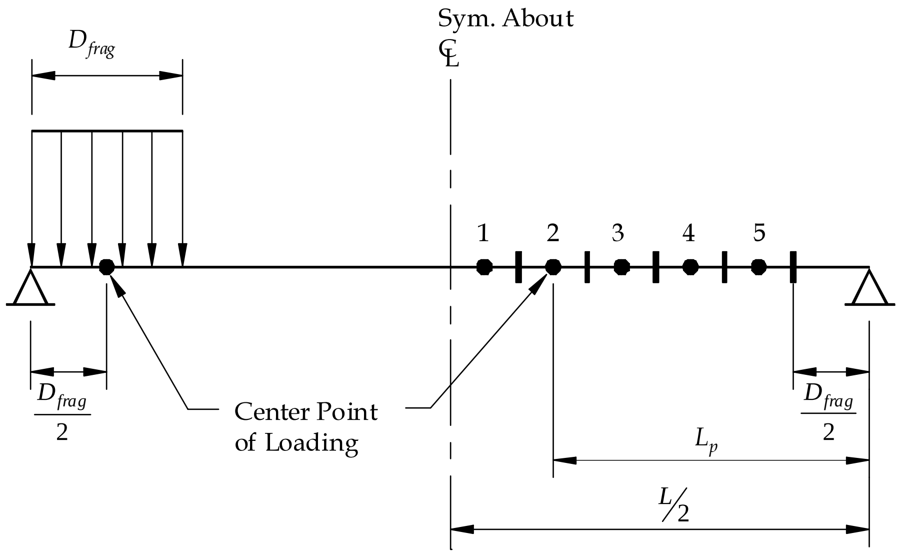

Figure 10. Distribution of loading center points across beam span.

$$E_{fail} = \frac{1}{2} R_y \left(\frac{R_y}{K} \right) + R_y \left(D_{max} - \frac{R_y}{K} \right)$$

$$V_r = \sqrt{V_{frag}^2 - \left(\frac{2E_{fail}}{M} \right)}$$

where *Vr* is the residual velocity and the SDOF parameters are those defined in Figure 9. A similar approach was used for the empirical and shear energy models; since these computed the fragment velocity required for penetration V_{pen}, the above equation was modified as follows:

$$V_r = \sqrt{V_{frag}^2 - V_{pen}^2}$$

Failure and Hazard Areas

If a structural member does fail, what portion of the roof or floor fails with it? To determine the failure area of the roof/floor structure, it is necessary to distinguish between plate and joist/girder failure and between shear and flexure failure modes; the failure areas implemented in HACK are sketched in Figure 11. For shear punch-through of the plate, it was assumed that the failure occurred nearly along the perimeter of the fragment, so that the portion of roof structure that came down was equal to the fragment area. However, if the plate failed in bending, a strip of plate equal in width to the fragment width and having the length of the joist spacing was assumed to fail. For joists and girders, failure (whether in flexure or shear) was assumed to cause failure of all framing elements supported by that member. Hence, if a joist fails, the plate on either side will also fail as far as the next adjacent joist; if a girder fails, all joists framing into that girder will also fail, as well as the plate framing into those joists.

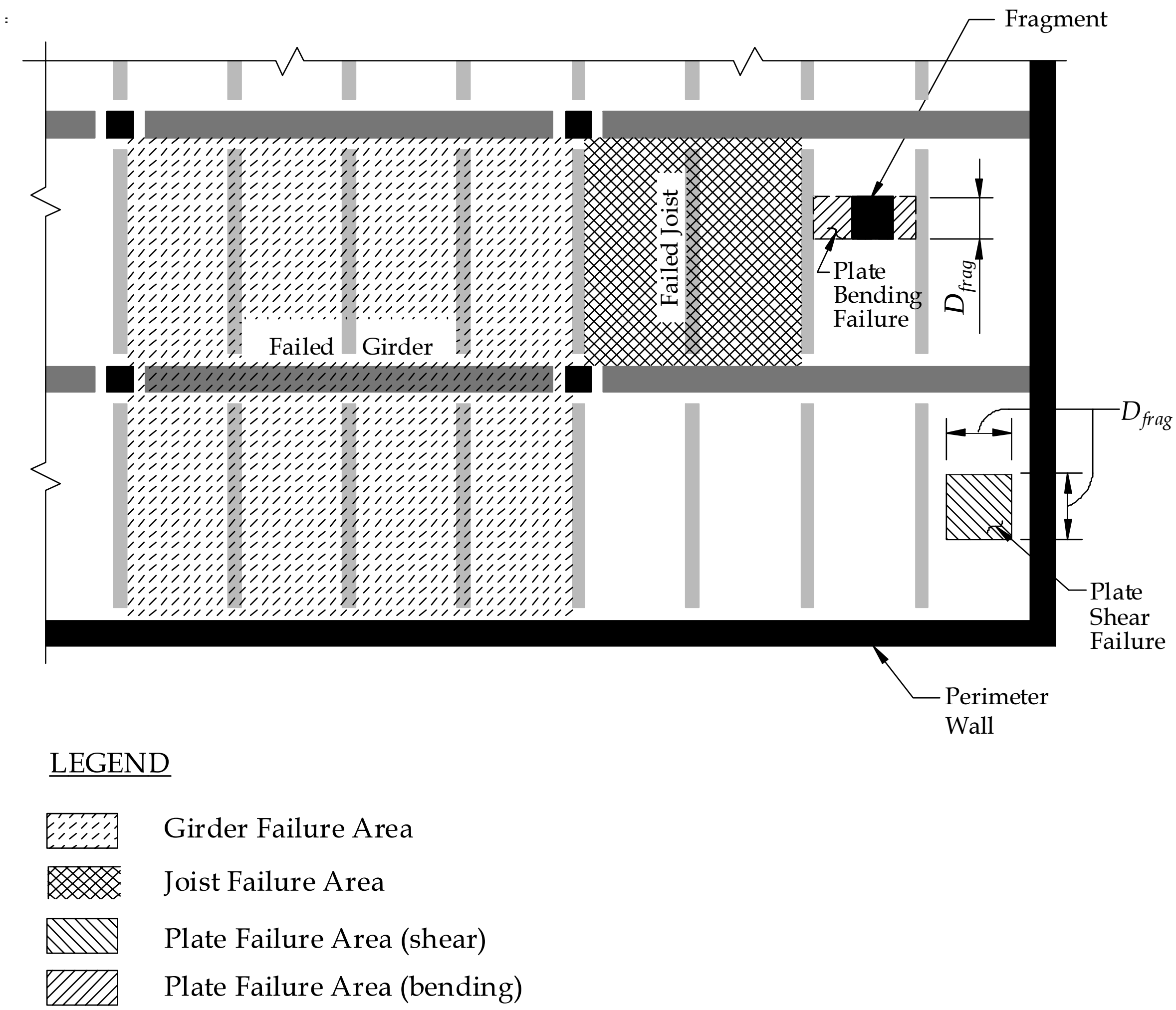

Figure 11. Definition of failure areas.

But what happens to all this debris as it comes down from the roof to the floor? Certainly some dispersion of the debris will occur due to the non-uniformity of the response and the energy of the impact, so that the actual hazard area is likely to be significantly greater than the failure area. To account for this effect, a factor F_{dam} was introduced which, when applied to each dimension of the failure area, produced the hazard area on the next floor level, as shown in Figure 12; the actual factor on the area is thus $(F_{dam})^2$. The values of F_{dam} used were varied depending on the type of failure: for shear failures a value of 1.5 was used while 2.0 was used for bending. This accounts for the fact that bending failures are the result of hinge formation and significant rotations of the structural members, so that the spread of secondary debris is likely to be greater than for a relatively “clean” shear failure.

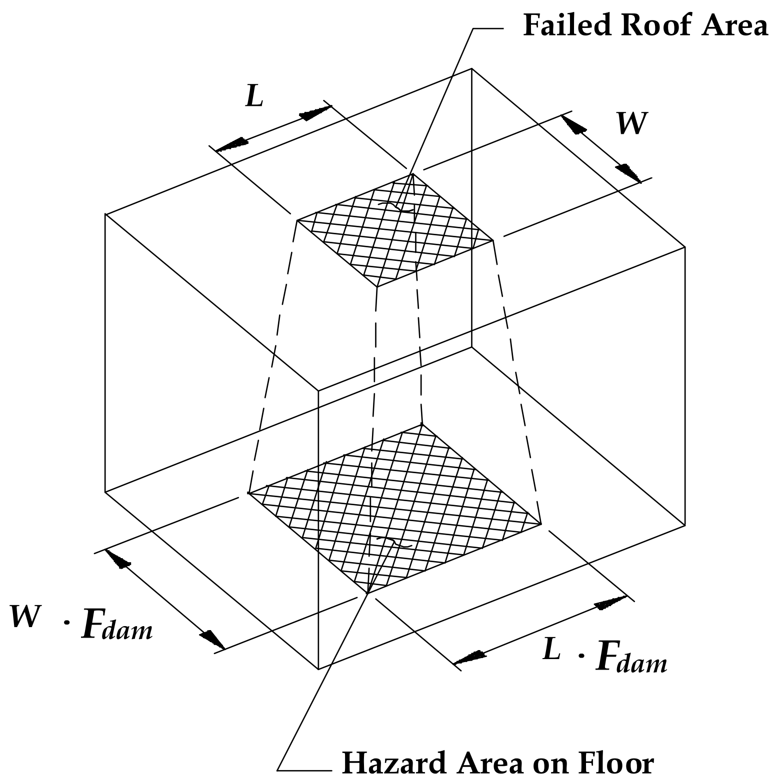

Figure 12. Factor F_{dam} to account for debris dispersion.

Sample Results

To verify the functionality of HACK and to examine the parametric sensitivity of its results, a series of sample problems were analyzed. One set used a typical steel building, 180 by 120 feet in size, with steel girders and joists and ribbed roof decking as shown in Figure 13; for simplicity, it was assumed that the building only had a single story. A small fragment weighing 42 pounds and with an area varying between 50 and 100 square inches was used in the analyses, the impact velocity being varied as an independent parameter against which the hazard area could be assessed.

A summary of the hazard area for this building/fragment combination as a function of impact velocity is presented in Figure14. Since the intent of the exercise was to evaluate the model's response, the velocity was increased beyond realistic limits for falling debris. The curve clearly demarcates the various regimes of plate, joist, and girder failure as well as the distinctions between shear and bending failure, with the associated variations in hazard area.

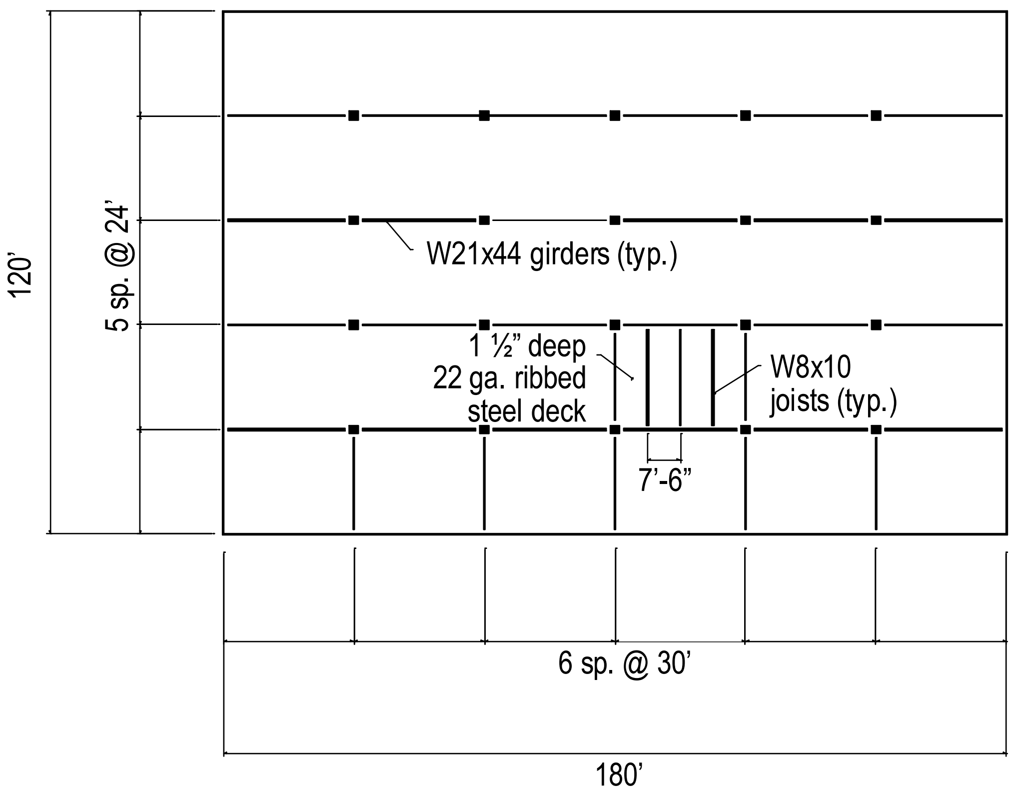

Figure 13. Steel building used for verification analyses.

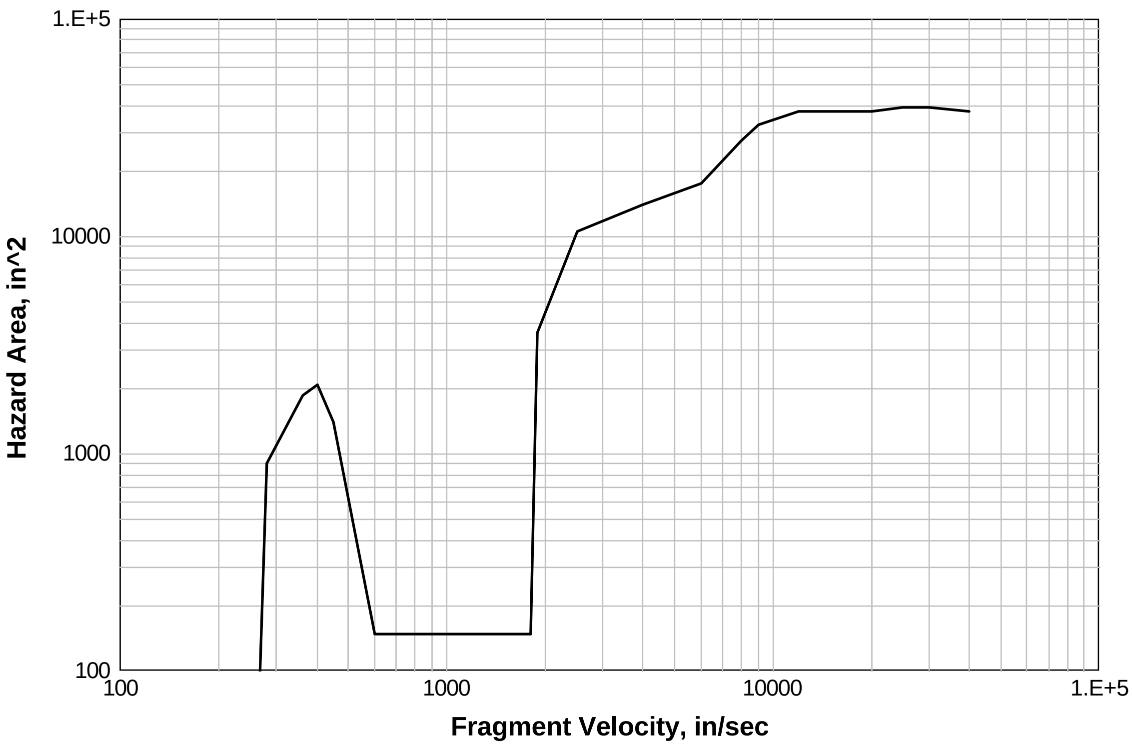

Figure 14. Hazard area as a function of fragment velocity for a typical steel building.

Initially, for very low velocities, the hazard area is 0; as the velocity reaches 280 in/sec, plate *bending* failure begins to happen with increasing probability, hence the gradual increase in hazard area. However, as the velocity tops 400 in/sec, plate *shear* failure begins to happen for the smaller fragment areas; as the velocity reaches 600, shear failure now happens for all areas. The reduction in hazard area is consistent with the assumed failure areas shown in Figure 11: plate shear failure only creates a failure area equal to the fragment area (quite small in this case), while bending failure causes failure of an entire strip spanning between joists. An additional factor is the differing value of $(F_{dam})^2$ which is 2.25 for shear and 4.0 for bending. Between 600 and 1800 in/sec, there is no change since the plate consistently fails in shear while the joists and girders remain unharmed. However, beyond 1800 joist bending failures begin to occur with increasing probability until, at 6000, there is joist failure in all cases. Since the failure area for joists is significantly greater than that for plate, the hazard area at these velocities is also greater. Beyond 6000 in/sec, girders begin to fail in bending, though the probability of such failures never exceeds 0.8 (i.e., impact near the support never causes failure). It is interesting to note that even though the failure area associated with girders is very large, the probability of impacting a girder is very small (compared to the probability of impacting the plate which occupies a much larger area). Consequently, the effect on hazard area of girder failures is relatively minimal. Finally, at very high velocities (from 30,000 to 40,000), some joist *shear* failures begin to occur, which (due to the variability of F_{dam}) results in a slight decrease in the hazard area. This is consistent with our intuition, since we would expect very high-velocity fragments to shear through whereas slower ones would be more likely to excite bending modes.

To evaluate the functionality of the code for a multi-story building, a 6-story building was defined using the roof structure in Figure 13 for all the floors as well; a different fragment was used in these analyses, one weighing 760 pounds and having an area varying from 1000 to 4464 square inches. The results, shown in Figure 15, are consistent with our expectations. For low velocities, the fragment penetrates the roof and causes hazard areas on the top floors, but the gradual decay of velocity prevents the lower floors from being affected. Gradually, as the velocity is increased to 700 in/sec, significant levels of hazard area are observed even on the lowermost floor, indicating that in *some* of the scenarios analyzed, the fragment was able to penetrate all the way to the bottom. The reversal in hazard area as a function of velocity observed in Figure 14 is seen here as well: for the top floor, going from 700 to 1000 in/sec reduces the hazard area, though the magnitude of the decrease is much less than it was for the smaller fragment used earlier. This too is consistent with expectations, since the larger fragment will produce a larger failure area during plate punch-through, and the contrast between plate shear and bending failures will not be as drastic. Returning to Figure 15, as the velocity is raised to sufficiently high levels, failure occurs for all elements and the attenuation of velocity is too slight to make any difference; hence, the hazard area is constant over all floors[6].

[6] Similar verification problems were devised in which the concrete and wood options were exercised; in all cases, the observed behavior was consistent with the idealizations implicit in the model and was generically similar to the steel building results shown above.

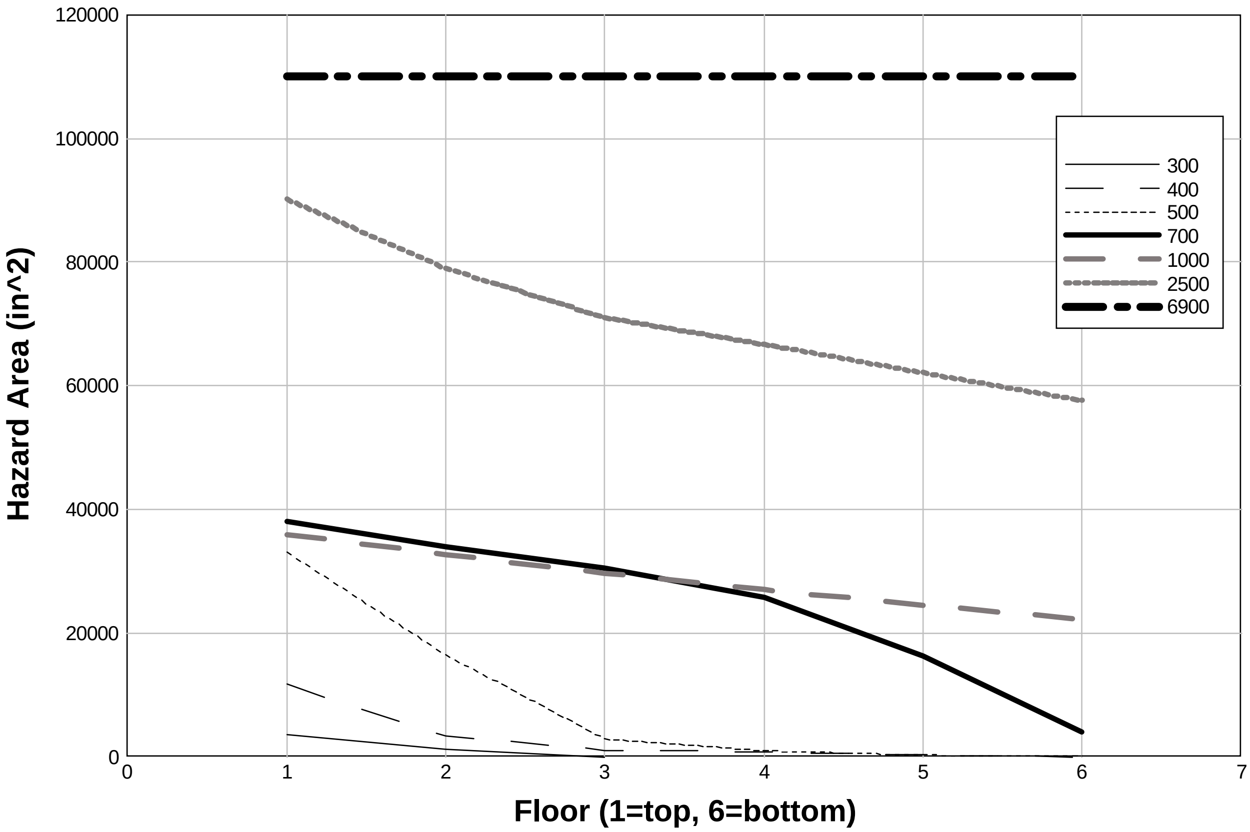

Figure 15. Hazard areas for typical multi-story steel building.

Conclusions

In summary, a simple yet rational model has been developed which permits the development of quantitative hazard assessments for generic fragments falling upon generic conventional buildings. User inputs are limited to the basic quantities available to analysts and engineers, and the output reflects the probabilities associated with impact upon each type of structural member and failure of that member. The modular construction of the model permits components to be easily inserted as new test data becomes available and/or new analytical methods are developed.

This approach provides an example of how hazards such as fragment impact can be propagated within a structure with regard to basic physics yet without undue computational effort. A similar approach could profitably be applied to the propagation of other hazards such as blast and contaminants to allow risk assessments of buildings which include the effects of building contents.

Acknowledgment

The authors wish to acknowledge the 30th Space Wing Flight Safety Analysis Office (SEY), Air Force Space Command, Vandenberg Air Force Command, under whose sponsorship the above model was developed.